((please add journal code and manuscript number, e.g., DOI: 10.1002/ppap.201100001))
Article type: Full Paper

Single-Stage Plasma-Chemical Synthesis and Characterization of Carbon Nanoparticle – Polymer Suspensions [a]

Dedicated to the blessed memory of our teacher and colleague, Prof. Dr. Yury Ehilevich Polsky (1931-2018).

Corresponding authors: Maxim P. Danilaev*, Iskander R. Vakhitov*

_____

Prof. M. P. Danilaev, Dr. E. A. Bogoslov, V. A. Kuklin,
Kazan National Research Technical University named after A.N. Tupolev – KAI, Kazan, 420111 Russia
E-mail: Danilaev@mail.ru
I. R. Vakhitov, Dr. V. G. Evtyugin, B. Z. Kamaliev, Dr. I. V. Lunev, Yu. N. Osin, A. M. Rogov
Institute of Physics, Kazan Federal University, Kazan, 420008 Russia
Prof. L. R. Tagirov
E.K. Zavoisky Physical-Technical Institute, FRC Kazan Scientific Center of RAS, Kazan, 420029 Russia;
Institute of Physics, Kazan Federal University, Kazan, 420008 Russia

_____

Thin-film styrene polymer – carbon nanoparticle composite was obtained in a single-stage alternating current dielectric barrier discharge plasma-chemical process. The allotropic forms of the carbon nanoparticle filler were traced by the Transmission Electron Microscopy. The TEM revealed an extraordinary adhesive encapsulation of the carbon nanoparticles by the polymer. It was found that the corona discharge regime provides an onion-like carbon filler that enhances the mechanical strength and chemical resistance of the synthesized polymer-

[a] ((Other reference to the authors can also appear here, such as Author-One and Author-Two contributed equally to this work.))

carbon nanoparticle film. Measurements of the electrical properties of the films implicitly confirmed the uniformity of the carbon filler distribution.

Keywords: AC barrier discharges; adhesion; encapsulation; plasma-chemical synthesis; polymer-carbon composite

1 Introduction

One of the main problems in preparation of polymer composites filled with carbon nanoparticles is the low reproducibility of their physico-chemical properties. [1–3] The most common reason is poor wettability of carbon particles by polymer, which leads to the agglomeration of these particles and their non-uniform distribution throughout the material.[4,5] The main approach to solve this problem is functionalizing the surface of carbon particles, for example, by chemical grafting of hydroxyl groups [6,7] or forming a shell on surfaces of the particles.[8-10] These procedures require the introduction of additional operations into the workflow for the pre-treatment of filler particles. At the same time, there is a method for producing polymeric coatings utilizing gas-discharge plasma, which allows synthesis of carbon particles directly in the process of the polymer formation.[11,12] It was shown in our preliminary studies that it is possible to obtain a more uniform distribution of carbon particles in the polymer matrix,[11] compared with the conventional methods of their introduction.[4,5] The gas discharge technique forms a shell, for example, an oligomer or polymer on the particles surface corresponding to the initial monomer.[11] Such a shell can enhance the adhesion of particles to the polymer matrix, and, as a result, significantly affects the mechanical characteristics of the polymer compositions.[10] In the paper we report on single-stage, dielectric barrier discharge (DBD) plasma synthesis of the polystyrene – carbon nanoparticles compositions and their physico-mechanical characterization.

2 Experimental Section. The samples synthesis

The experimental setup for synthesis of polymer-carbon nanoparticle composites utilizes atmospheric pressure AC dielectric barrier corona discharge.[11,13,14] The particular scheme of the installation (plasma-chemical reactor) is shown in **Figure 1**.

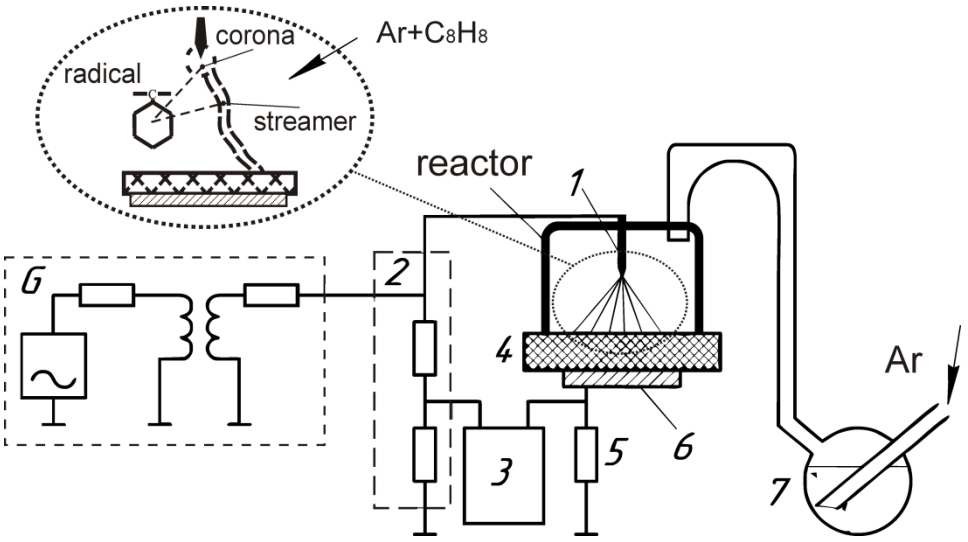

Figure 1. Scheme of the experimental setup: *1* –corona electrode; *2* –circuit; *3* – feedback block; *4* – substrate; *5* – limiting resistor; *6* –counter electrode; *7* – bubbler.

The DBD corona plasma of alternating (40 kHz) current was created by the coronator *G* (KP1-300) at the needle *1* – plane counter electrode *6* system. The average electric field strength was controlled in the range of 6 – 20 kV cm^{-1} with an accuracy of ± 0.5 kV cm^{-1} and is determined as the applied voltage divided by a distance between the needle *1* and the counter electrode *6*. Ceramic tile *4*, 3 mm thick, served as a dielectric barrier. The distance between the needle and the barrier was varied in the range 10 – 20 mm with an accuracy of ± 0.5 mm. The voltage at the electrodes of the plasma-chemical reactor was measured using a voltage divider *2* and recorded with an oscilloscope *3* (ACK-2205). A copper electrode of 75×75 mm^2 dimensions was used as a flat counter electrode *6*. The discharge current was controlled by measuring the voltage drop on the calibrated shunt *5* and also recorded with an oscilloscope *3*. Typical oscillograms of the discharge current are shown in Figure 2. A polymer film was formed on the surface of the barrier plate *4* from the styrene vapor, fed into

the plasma-chemical reactor from the bubbling device *7*. High-purity argon was supplied as a carrier gas from a cylinder through a pressure reducer at the pressure *p* in the range 1000–1200 hPa with an accuracy of ± 5 hPa. The flow rate in the range of ~ 6-360 ccm/min provided the content of styrene vapor in the plasma chemical reactor of about 0.3-17 g/m^3 (±10%).[15] For the particular sample preparation these parameters were 350 ccm/min and 16.6 g/m^3, respectively. The ignition threshold voltage of the corona discharge for the needle – plane electrode system was ~ 5.5–6 kV at the gap size of 20 mm. The discharge power was controlled in the range 100-300 watts with an accuracy of 10%.

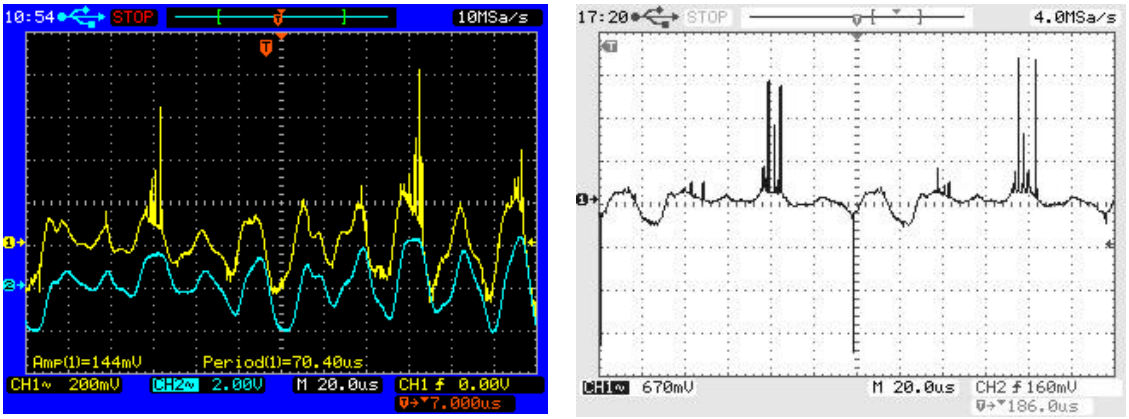

Figure 2. Left – oscillograms of the applied voltage (light blue) and the discharge current through the resistor *5* (yellow) taken at the electric field strength $|E| < E_0$ (see below); right – oscillogram of the discharge current through the resistor *5* (yellow) taken at the electric field strength $|E| > E_0$.

The use of a sharply inhomogeneous electric field near the needle and the flow of a corona discharge in the presence of monomer vapor (styrene) in the gaseous medium initiate the formation of radicals (shown by the callout drawing in Figure 1) and trigger a radical polymerization mechanism on the surface of the dielectric barrier.[16] At the same time, the temperature of the two-phase medium increases in the discharge flame, and formation of carbon particles begins when the temperature reaches ~ 600–950°C.[17,18] The mechanism of the carbon particles formation is based on the thermal destruction of monomer molecules in areas with high current density and, consequently, temperature.[13]

In the AC DBD discharge, two such regions are distinguished.[17,18] The first one is a corona shell located around the needle *1* (see Figure 1), it appears above the discharge ignition voltage ~ 5.5–6 kV. Heat generation in this zone occurs mainly at a negative potential on the needle. This area has nearly spherical shape with an outer diameter of around 0.5-1 mm and the inner diameter of ~ 0.1 mm apart from the surface of the corona-forming electrode.[14,19] The second region, the streamer, arises at sufficiently high electric field strengths E = 7-8 kV cm^{-1}, it turns into a spark with increasing of E.[19,20] The characteristic duration of the streamer in our experiments was ~ 10^{-8}–10^{-5} s. The heat is generated from such an energy source in a small volume restricted to the length of the discharge gap and a streamer cross section that does not exceed the size of the avalanche head at the stage of its largest expansion, ~ 0.1–1 mm.[21]

The allotropic form of carbon particles formed in the discharge area depends on the absolute value of the temperature in the corresponding region.[22] The temperature is different in the first and second discharge areas and is determined by the electric field strength via the current density, and the monomer vapor concentration in the plasma-chemical reactor.[18-21] Therefore, it is likely that the allotropic form of carbon particles formed in these regions could differ. The average temperature was estimated in the framework of the model with a point (for the corona), linear (for the streamer) and instant heat source, in the approximation of the frozen parameters of the medium.[23] The initial guesses for the modeling were determined from the measured parameters (amplitude and duration) of the discharge current pulses for a given electric field strength, they varied within 0.2–1.5 A for the current amplitude and 0.3–1.5 μs for the pulse duration.

Average values of temperature in the first (T_1) and second (T_2) areas are shown in **Figure 3**.

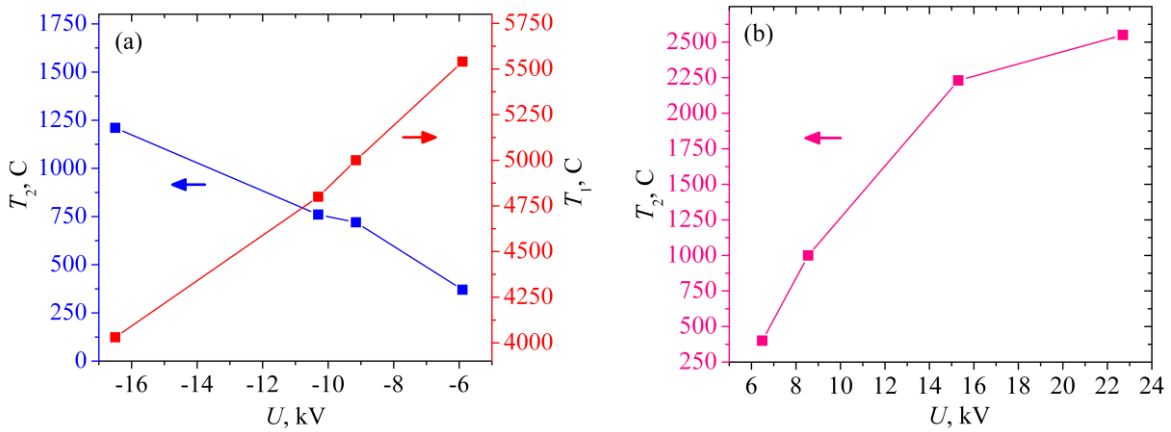

Figure 3. Dependence of the average temperature in the first region – T_1, and in the second region – T_2, on the applied voltage: a) the negative potential φ on the corona electrode (needle); b) the positive potential φ on the corona electrode (needle). The lines connect the points.

In the first region, the range of temperatures 4000–5500°C obtained from our modeling (Fig. 3(a)) is suitable to form fullerenes and similar particles, for example, "onion-like carbon" in the entire range of the electric field strengths.[22] In the second region, the lower temperature limit ~ 600–950°C, starting from which the formation of carbon particles is possible, corresponds to the electric field strength $|E| > E_0$, where E_0 ~ 7-8 kV cm^{-1}. At temperatures of 600–2500°C in this region, the formation of both amorphous carbon black particles and structured carbon particles, such as carbon black crystallites and graphite particles, is possible.[13,22] The non-linear dependence of T_2 versus applied voltage, Fig. 3(b), is a consequence of the nonlinear current-voltage characteristic of the plasma.[14] The variety of allotropic forms of carbon particles in a polymer film increases with increasing $|E|$ above E_0, since the temperature in the corona shell remains sufficient for the formation of fullerenes and similar particles. Thus, a corona DBD in the presence of monomer vapor provides conditions for the formation of a polymer film with the simultaneous formation of carbon particles embedded into this film.

To identify the allotropic form of the carbon nanoparticles synthesized in a polystyrene film as described above, two series of samples were prepared. The first series of

samples was obtained at the corona discharge regime at electric field strengths $|E| < E_0$. Thus, the source of carbon particles in this series of samples is only the corona shell. The second series of samples was obtained at electric field strengths $|E| > E_0$, when streamers appear in the discharge plasma. In this case, carbon particles were formed simultaneously in both regions with elevated temperatures: corona shell and streamers. Typical conditions under which samples were obtained are as follows:

- Sample 1: $|E| = 6.8 \pm 0.5$ kV cm^{-1}; the pressure *p* of argon gas with monomer vapor at the entrance to the plasma-chemical reactor, $p = 1010 \pm 0.5$ hPa; the distance between the electrodes is 20 mm; the film deposition time – 2 min;

- Sample 2: $|E| = 10 \pm 0.5$ kV cm^{-1}; the pressure *p* of argon gas with monomer vapor at the entrance to the plasma-chemical reactor, $p = 1010 \pm 0.5$ hPa; the distance between the electrodes is 20 mm; the film deposition time – 2 min.

The sample films were deposited on a thoroughly cleaned cover glass (microscopic coverslip) of the 20×20 mm^2 square shape with a thickness of 0.1 mm, the average thickness of the film ~ 0.5 μm. The thickness of the polymer films was measured with a Bruker DektakXT™ (USA) nanoprofilometer (the stylus radius is 2 μm, the application force – 3 mg) with accuracy not worse than 10 nm.[15]

3 Characterization Results and Discussion

3.1 Identification of the allotropic form of carbon particles by transmission electron microscopy

The identification of allotropic forms of carbon particles formed at various electric field strengths in the polymer films was carried out utilizing a transmission electron microscope (TEM) Hitachi HT7700 Exalens at the acceleration voltage of 100 kV by visualizing

individual particles and analyzing the electron diffraction on these particles. For the TEM studies, a liquid suspension of carbon particles was prepared by dissolving the polymer film in acetone (99.9%) during 20 minutes. As a next step, the resulting solution was actuated in an ultrasonic bath at least 10 minutes at the frequency of 44 kHz and the ultrasonic power of ~10 W. The morphology of the washed up carbon inclusions was studied before and after the ultrasonic actuation as well.

TEM images of carbon particles prepared without ultrasonic dispersing are shown in **Figure 4**. A clearly visible halo around the particles and their agglomerations represents polymer shells which remain unpeeled in a still acetone of 99.9% purity even for 48 hours.

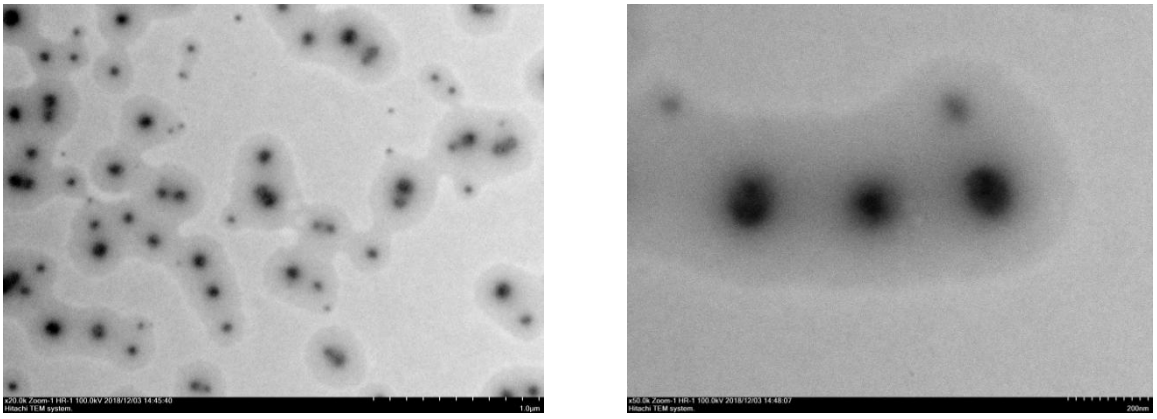

Figure 4. Typical micrograph of carbon particles from Sample 1 for the case of the probe preparation without ultrasonic dispersing (two magnifications are shown: ×20k – left, and ×50k – right).

The characteristic thickness of these shells has the order of the size of carbon particles themselves. The presence of the polymer shell on the particles after dissolving the film in the solvent indicates an unusually strong crosslinking of the polymer molecules nearby the carbon particles and possible enhanced adhesion between the polymer molecules and carbon particles,[24] however, we do not have direct characterization for the latter.

The polymer shells of carbon particles can be completely removed only after ultrasonic exposure to a solution of the film in acetone. Typical micrographs and electron diffraction patterns of the carbon particles formed in polymer films of the Sample 1 series are shown in **Figure 5**, while of the Sample 2 series – see **Figure 6**.

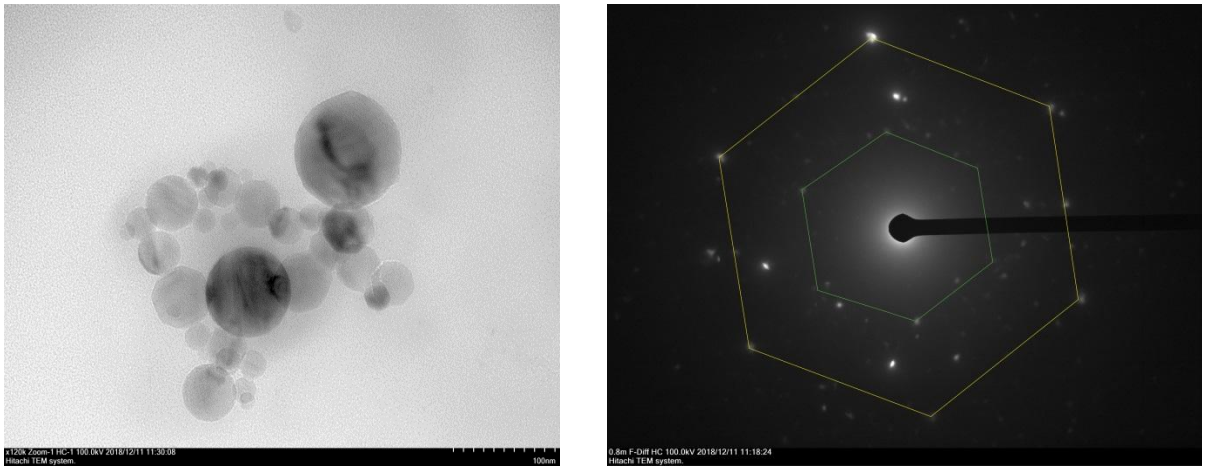

(1) (2)

Figure 5. Typical micrograph (1) and electron diffraction (2) of the carbon nanoparticles from Sample 1. A hexagonal motif along the [0001] zone axis of the spots layout is shown by color hairlines.

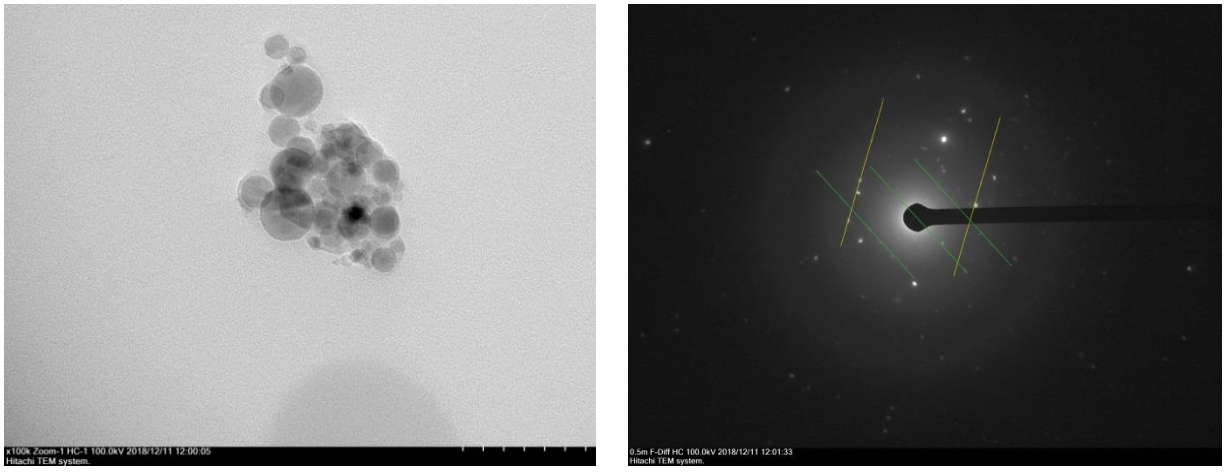

(1) (3)

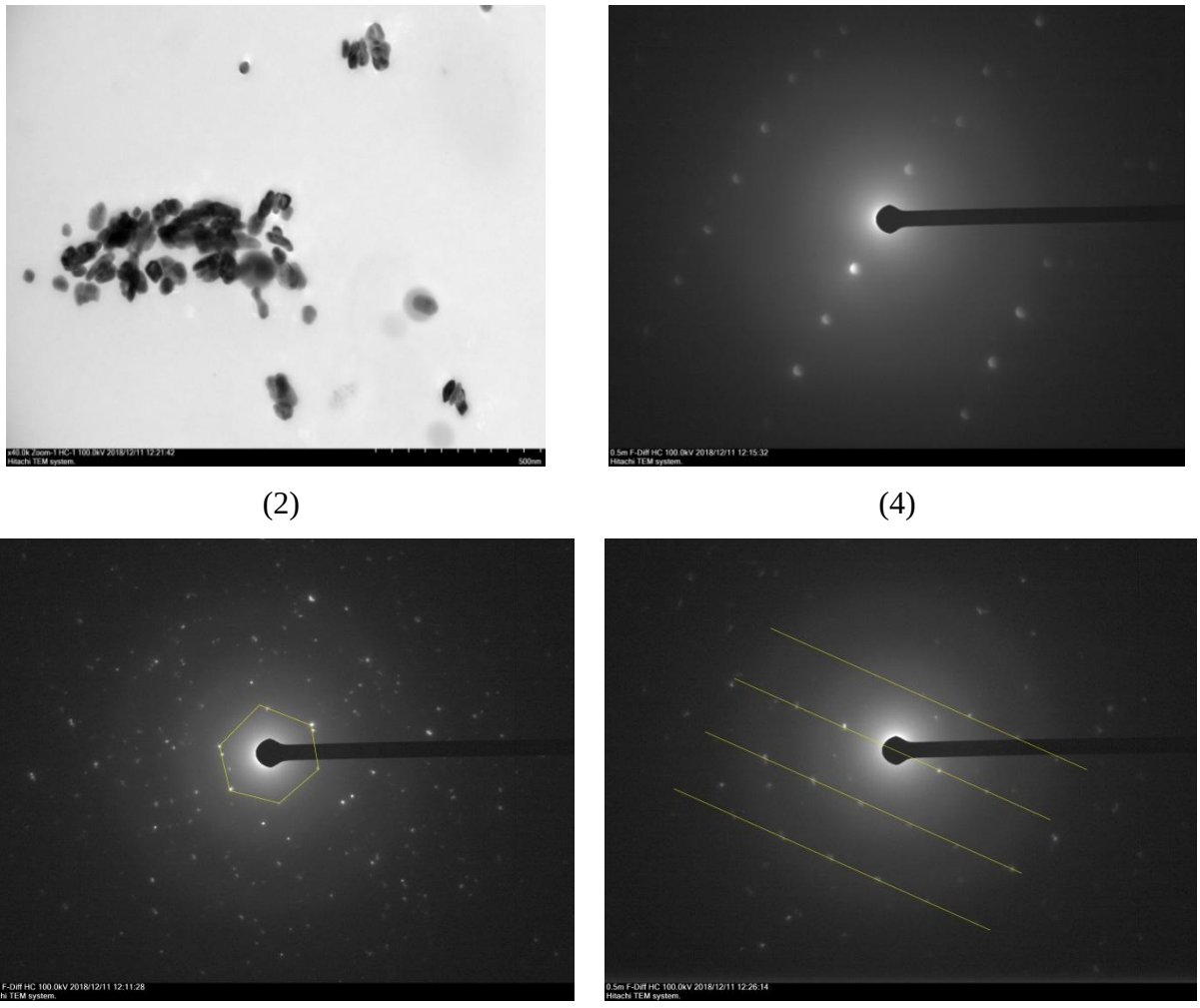

Figure 6. Typical micrographs: fullerene-like particles (1) and diffraction of electrons from fullerene-like particles (3); structured carbon particles (SCP) (2) and electron diffraction for SCP (4)-(6) extracted from Sample 2. The guide for the eye hairlines are explained in the text.

Diffraction rings in Figure 5(2) and Figures 6(3)-6(6) correspond to the carbon substrate on which the samples were deposited. To analyze the electron diffraction reflexes the method described in Refs. [25–28] applies. In a more illustrative way for hexagonal lattices the electron diffraction patterns analysis was presented in Ref. [29]. Figures 5(1) and 6(1) shows agglomerates of fullerene-like nanoparticles or onion-like carbon the electron diffraction patterns of which look quasi-random (Figures 5(2) and 6(3)).[26,28] Nevertheless, it is possible to separate out from the others the reflexes of hexagonal structure along [0001] zone axis (not completely perfect), marked in Figure 5(2) by green and yellow hairlines (compare with Figure 2(a) of Ref. [29]). On the contrary, the ordered pattern in Figure 6(3) contains chains

of spots (marked by yellow and green hairlines) which nevertheless can be identified with the hexagonal structure, however, for diffractions along the $[11\bar{2}1]$ (green) and $[41\bar{5}0]$ (yellow) zone axes, respectively (see Figures 2(c) and 2(d) of Ref. [29]), both perpendicular to the hexagonal *c*-axis [0001].

Figure 6(2) presents the image of arrangement of the agglomeration of carbon particles, most of them looks like crystallites. The electron diffraction patterns in Figures 6(4)–6(6) correspond to multilayered graphene structures (graphite sheets) or to carbon black crystallites.[29,30] Indeed, patterns 6(4) and 6(6) obtained from well-defined crystallites look very much like taken along $[41\bar{5}0]$ zone axis (Figure 6(4), compare with Figure 2(d) of Ref. [29]), and along $[11\bar{2}1]$ zone axis (Figure 6(4), compare with Figure 2(c) of Ref. [29]) with correct relationship for distances between the spot chains. Image 6(5) taken from the dark area of the agglomeration shows superposition of randomly oriented but crystalline scatterers, however, the hexagonal motif (slightly distorted) can be identified at the center of the zone (shown in thin yellow lines).

The TEM results support the existence of two regions in a barrier corona discharge with different temperatures: the onion-like carbon nanoparticles form in the area around the corona electrode – in the corona shell, while crystallized carbon black agglomerates and/or multilayered graphite sheets – in the streamers.

3.2 The study of polymer films by scanning probe microscopy

The morphology of the polymer film with carbon particles, the assessment of the size range of carbon particles under various conditions of their formation, as well as the compression deformation mapping were carried out using scanning probe microscope Dimension Fastscan by Bruker (Germany).[31,32] The morphology of the polymer films surface is shown in **Figure 7**.

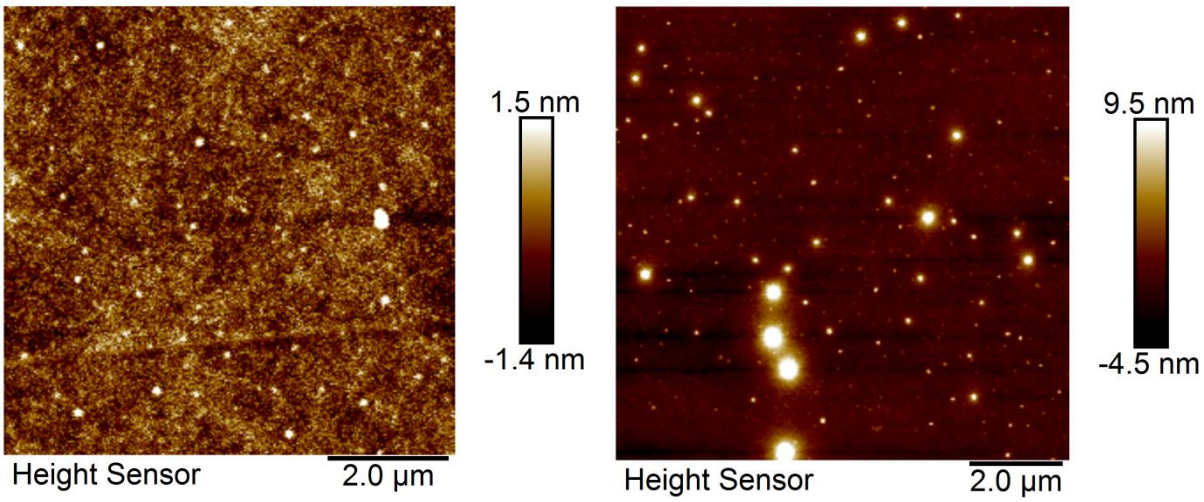

(1) (2)

Figure 7. Morphology of the polymer films: (1) – Sample 1; (2) – Sample 2. White spots are carbon nanoparticles that protrude above the mean surface of the film.

The distribution of carbon particles in polymer films Sample 1 and Sample 2 are uniform with the size range covering: 80–400 nm – in Sample 1; 40–600 nm – in Sample 2. The specific concentration of carbon particles in the samples is close to each other and equals to ~ 7×10^{8} cm^{-2}. This corresponds to their volume fraction of ~ 10^{-2}%.

It should be noted that the adhesion of particles to the polymer film is not uniform over the film surface (see **Figure 8**). It is possible that allotropic modification as well as non-equilibrium temperature upon reaching the substrate surface could influence the bonds formation between carbon particle and polymer molecules as well as the C–C distance.

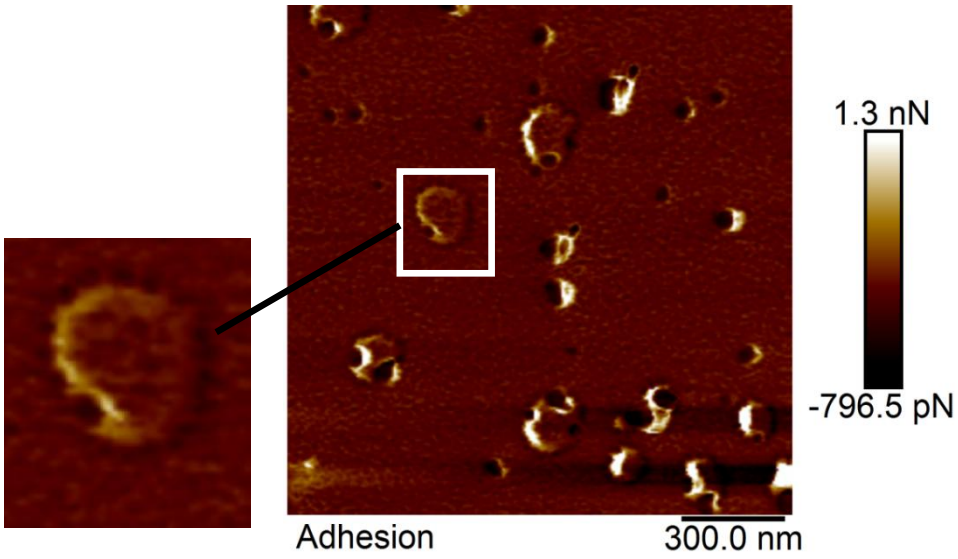

Figure 8. Typical pattern of the carbon particles adhesion to the polymer film (Sample 2).

To determine the effect of carbon particles on the physico-mechanical properties of the deposited films, we investigated the compression deformation of the films in their transverse direction and their dielectric properties. The mapping of the deformation of the samples was carried out on the Bruker Dimension Fastscan microscope in a mode of quantitative nanomechanical mapping. The Bruker scan-assist Air cantilevers were used with a stiffness of 0.4 N m^{-1} and a radius of curvature of ~ 5 nm. The probe-sample interaction force was maintained by feedback at a value of 5 nN. A comparative analysis of the strain (**Figure 9**) shows that the strain value increases for the films obtained at higher electric field strengths $|E| > E_0$. The ratio of the mean strain values for Sample 1 (δ_1, pm) and Sample 2 (δ_2, pm) is δ_1 / δ_2 ; 0.29. Based on our previous studies we refer this feature to a higher density of cross-links at low deposition rates.[15,33] In a result, the Sample 1 film (Figure 9(a)) deposited at lower deposition rate gets harder compared with the Sample 2 film (Figure 9(b)) deposited at higher rates.

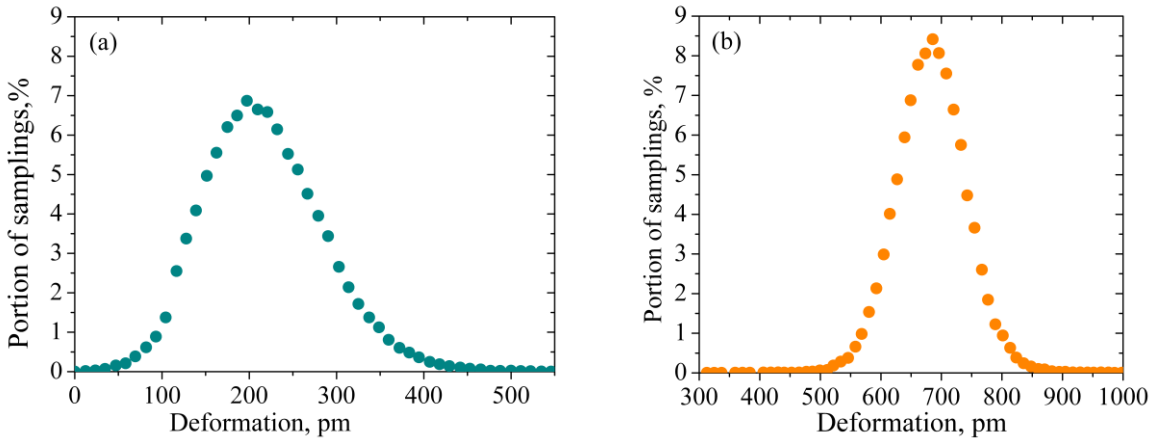

Figure 9. Statistics of deformations of the surfaces of Sample 1 – (a), and Sample 2 – (b) under measurement conditions given in the text.

3.3 Study of electric properties of polymer films by dielectric spectroscopy

The dielectric properties of polymer films with carbon particles were studied by dielectric spectroscopy utilizing Novocontrol BDS-80 (Germany) spectrometer. Two schemes were used to measure the specific dielectric characteristics of the films: transverse, when electrodes sandwich the film; and longitudinal, when the electrodes are attached to the opposite edges of the film.[34] The transverse measurement scheme allows one to determine the electrical properties of the carbon particles themselves, because carbon particles protrude above the surface of polymer films (see Figure 7). To get access to carbon from below, it is necessary to use a conductive substrate (see below). In the longitudinal measurement scheme, the dielectric properties of polymer films filled with carbon particles (polymer-carbon composite) are measured.

For the dielectric spectroscopy studies, a special set of samples was prepared in a single run. Realizing the transverse scheme of measurements, finely polished and thoroughly degreased and washed brass substrate of 25 ± 0.2 mm in diameter was placed on the dielectric barrier *4* (see Figure 1) together with the cover glass substrate for the longitudinal scheme of measurements. After preparation of a polymer film, a top electrode for the transverse measurements was deposited onto the polymer film surface on the brass by spraying a

conductive paint containing copper nanoparticles through a mask. The top electrode diameter was ~ 10 mm, and the brass substrate served as the lower electrode at electric measurements.

To study dielectric properties in the longitudinal measurement scheme, the electrodes were deposited on the upper surface of the film on the glass utilizing the same mask technique. Two stripes of about 4 mm in width were formed along the opposite edges of the square substrate with the gap ~ 10 mm between them. This made it possible to study the dielectric properties of polymer films filled with carbon particles (polymer-carbon particle composite).

The polymer film preparation conditions were almost the same as in the Section "The samples synthesis" above, however, at little bit lower electric field strengths: $|E| = 6.3 \pm 0.5$ kV cm^{-1} – for the Sample 1 type (corona shell discharge regime), and $|E| = 9.3 \pm 0.5$ kV cm^{-1} – for the discharge regime with streamers. The discharge current upon receipt of these samples was within 10% deviations from the case of the samples for TEM and scanning probe microscopy studies.

The results of the measurements for Samples type 1 and 2 are presented in **Figure 10**. The scatter in the measuring of conductivity did not exceed 10%.

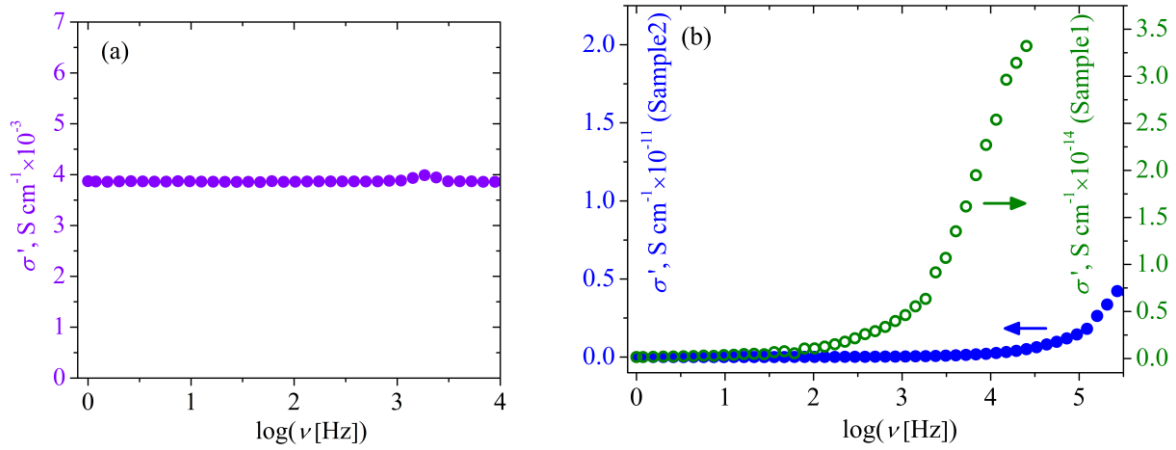

Figure 10. Frequency (ν) spectrum of specific conductivity of the polymer films with carbon particles; (a) – Sample 1 with the transverse measurement scheme, (b) – Sample 1 and Sample 2 with the longitudinal measurement scheme. The measurements temperature is 23 ± 0.5°C and the applied voltage – 0.5 ± 0.05 V.

In the transverse measurement scheme, the specific conductivity of carbon particles in our Sample 1 films was about 4×10^{-3} S cm^{-1} as it follows from Figure 10(a). For comparison, the conductivity of fullerene-like particles (onion-like carbon) can be estimated using the literature data, Refs. [35-37]. We postulate that the conductance of carbon particles in the samples sums additively, and assume that conductivity of fullerene-like particles (onion-like carbon) is higher than the conductivity of carbon black particles. Then, taking the low bound of the volume concentration of 10^{-2}%, estimated from analysis of our microscopy data, Figures 3 to 6, the average specific conductivity of the onion-like carbon particles can be assessed as being ~ 5×10^{-3} S/cm. This estimation corresponds to the results of our dielectric spectroscopy measurements in Figure 10a and implicitly confirms the assumption about onion-like carbon like origin of the carbon particles in our Sample 1 which follows from our TEM study.

For a reference, conductivity of fullerene C60 nanocomposite at a temperature of ~ 25°C lies in the range 10^{-8}-10^{-12} S cm^{-1};[35] the graphite powder conductivity – 1-10^{3} S cm^{-1};[36] the conductivity of carbon black depends on the method of preparation and lies in the range 0-10 S cm^{-1}.[37]

In the longitudinal scheme of measurements, the specific conductivity σ' of the polymer composite, uniformly filled with carbon particles at a volume concentration of ~10^{-2}%, lies in the range 10^{-11}-10^{-15} S cm^{-1} and is determined by the allotropic form of carbon particles, as well as their characteristic dimensions.[35-39] The specific conductivity of our polymer films (Figure 10(b)) fits this range. This indirectly confirms the homogeneity of the distribution of carbon particles over the volume of the polymer films.

4 Conclusions

Experimental studies demonstrate the possibility of depositing the polymer films uniformly filled with carbon particles in the single-stage plasma-chemical synthesis utilizing the alternating current dielectric barrier corona discharge plasma at atmospheric pressure. The results of the experimental studies demonstrate that:

- formation of carbon particles is carried out in areas with a high density of discharge current: in the corona near the needle electrode and in the volume of the streamers. At the electric field strength $|E| < E_0$, E_0 : $7-8$ kV cm^{-1}, fullerene-like particles (onion-like carbon) are formed in the corona, the average size of them is about 200 nm. At $|E| > E_0$, amorphous particles of carbon black and its crystallites (multilayered graphitic sheets) are formed in the streamer region, with the average size of 350-400 nm; fullerene-like (onion-like carbon) particles – near the needle electrode. The average volumetric concentration of carbon particles in the polymer films is estimated as ~ 10^{-2}%;

- carbon nanoparticles are dressed in a polymer shell hardly soluble compared with the film body. Solutions of such kind of polymer encapsulated carbon particles can be used to form dispersively filled polymeric materials with high adhesion of the filler particles to the polymer through the shell;

- the mechanical hardness (deformation on compression) of the polymer films obtained at lower electric field strengths $|E| < E_0$ is several times higher than that obtained at higher ($|E| > E_0$) strengths; based on our previous studies we refer this feature to a higher density of cross-links at lower deposition rates;[33]

- the results of transmission electron, atomic force microscopies and dielectric spectroscopy studies give evidence of uniform distribution of polymer encapsulated carbon nanoparticles in the samples obtained by alternating current dielectric barrier corona discharge plasma synthesis;

- for most of practical applications the polymer film coatings obtained in a gas discharge plasma at the synthesis conditions avoiding the formation of carbon black particles provide better physical-mechanical strength and chemical stability of the coating.

Acknowledgements: This work was supported by a grant from the Russian Foundation for Basic Research (RFBR No. 18-48-160024). The use of the KFU equipment facilities was partially supported by the Program of Competitiveness Growth of Kazan Federal University.

Received: ((will be filled in by the editorial staff)); Revised: ((will be filled in by the editorial staff)); Published online: ((please add journal code and manuscript number, e.g., DOI: 10.1002/ppap.201100001))

[1] S. Stankovich, D.A. Dikin, G.H.B. Dommett, K.M. Kohlhaas, E.J. Zimney, E.A. Stach, R.D. Piner, S.T. Nguyen, R.S. Ruoff, *Nature* **2006**, *442*, 282.

[2] A. Pantano, N. Montinaro, D. Cerniglia, F. Micciulla, S. Bistarelli, A. Cataldo, S. Bellucci, *Compos. Part B-Eng.* **2018**, *163*, 52.

[3] W. Khan, R. Sharma, P. Saini, "Carbon Nanotube-Based Polymer Composites: Synthesis, Properties and Applications", In *Carbon Nanotubes. Current Progress of their Polymer Composites* (Eds.M. Berber, I.H. Hafez), IntechOpen **2016**.

[4] H.S. Bedi, S.S. Padhee, P.K. Agnihotri, *Polym. Composite.* **2018**, *39*, E1184.

[5] M.Q. Tran, J.T. Cabral, M.S.P. Shaffer, A. Bismarck, *Nano Lett.* **2008**, *8*, 2744.

[6] *Chemical Science of π-Electron Systems* (Eds.T. Akasaka, A. Osuka, Sh. Fukuzumi, H. Kandori, Y. Aso), Springer Japan, Tokyo **2015**.

[7] L. Meng, Ch. Fu, Q. Lu, *Prog. Nat. Sci.* **2009**, *19*, 801.

[8] K.C. Hwang, *J. Phys. D: Appl. Phys.* **2010**, *43*, 374001.

[9] T. Li, J.F. Shen, N. Li, M.X. Ye, *Mater. Lett.* **2012**, *89*, 202.

[10] O.Y. Bogomolova, I.R. Biktagirova, M.P. Danilaev, M.A. Klabukov, Yu.E. Polsky, A.A. Tsentsevitsky, S. Pillai, *Mech. Compos. Mater*. **2017**, *53*, 117.

[11] E.A. Bogoslov, M.P. Danilaev, Yu.E. Polsky, M.S. Pudovkin, *Fiz. Khim. Obrab. Mater*. **2016**, *2*, 23 (in Russian).

[12] G. Raniszewski, S. Wiak, L. Pietrzak, L. Szymanski, Z. Kolacinski, *Nanomaterials* **2017**, *7*, 50.

[13] M.P. Danilaev, E.A. Bogoslov, Yu.E. Polskii, E.M. Zueva, M.S. Pudovkin, *Tech. Phys.* **2018**, *63*, 857.

[14] S.B. Afanas'ev, D.S. Lavrenyuk, I.N. Petrushenko, Yu.K. Stishkov, *Tech. Phys.* **2008**, *53*, 848.

[15] E.A. Bogoslov, M.P. Danilaev, Yu.E. Polsky, I.R. Vakhitov, A.I. Gumarov, I.V. Yanilkin, L.R. Tagirov, *Inorg. Mater.: Appl. Res.* **2018**, *9*, 385.

[16] *Plasma Polymerization* (Ed.: H.K. Yasuda), London: Academic, **1985**.

[17] T.S. Kol'tsova, T.V. Larionova, O.V. Tolochko, N.N. Shusharina, *Tech. Phys.* **2015**, *60*, 1214.

[18] D. Kozak, E. Shibata, A. Iizuka, T. Nakamura, *Carbon* **2014**, *70*, 87.

[19] Yu.K. Stishkov, A.V. Samusenko, I.A. Ashikhmin, *Phys.-Usp*. **2018**, *61*, 1213.

[20] *Gas Discharge Physics* (Ed.: Yu.P. Raizer), Springer, Berlin – New York **1997**.

[21] O.A. Omarov, A.A. Rukhadze, *Tech. Phys.* **2011**, *56*, 944.

[22] A. Szabó, C. Perri, A. Csató, G. Giordano, D. Vuono, J.B. Nagy, *Materials* **2010**, *3*, 3092.

[23] *A Heat Transfer Textbook* (Eds. J.H. Lienhard IV, J.H. Lienhard V), Phlogiston Press, Cambridge **2001**.

[24] Z. Marković, M. Kováčová, M. Mičušík, M. Danko, H. Švajdlenková, A. Kleinová, P. Humpolíček, M. Lehocký, B.T. Marković, Z. Špitalský, *J. Appl. Polym. Sci.* **2019**, *136*, 47283(1).

[25] *The Basic of Crystallography and Diffraction* (Ed.: C. Hammond), Oxford Science Publications, Oxford, **1997**.

[26] K. Hirahara, S. Bandow, K. Suenaga, H. Kato, T. Okazaki, H. Shinohara, S. Iijima, *Phys. Rev. B* **2001**, *64*, 115420.

[27] J.-F. Colomer, L. Henrard, P. Launois, G. Van Tendeloo, A.A. Lucas, Ph. Lambin, *Phys. Rev. B* **2004**, *70*, 075408.

[28] *Symmetry Relationships between Crystal Structures. Applications of Crystallographic Group Theory in Crystal Chemistry* (Ed.: U. Müller), Oxford University Press, Oxford **2013**.

[29] M. Feuerbacher, M. Heidelmann, C. Thomas, *Mater. Res. Lett.* **2014**, *3*, 1.

[30] T. Kamimoto, M. Yagita, *SAE Preprints* **1989**, *890436*, 9.

[31] S. Bellucci, G. Gaggiotti, M. Marchetti, F. Micciulla, R. Mucciato, M. Regi, *J. Phys. Conf. Ser.* **2007**, *61*, 99.

[32] R.N. Jagtap, A.H. Ambre, *Indian J. Eng. Mater. S.* **2006**, *13*, 368.

[33] M.P. Danilaev, E.A. Bogoslov, Yu.E. Polskii, I.V. Yanilkin, I.R. Vakhilov, A.I. Gumarov, and L.R. Tagirov, *Inorg. Mater.: Appl. Res.* **2019**, *10*, 556.

[34] *Dielektrische Messmethoden* (Ed.: F. Oehme), Weinheim/Bergstr, **1958**.

[35] S. Bronnikov, A. Podshivalov, S. Kostromin, M. Asandulesac, V. Cozanc, *Phys. Lett. A* **2017**, *381*, 796.

[36] B. Marinho, M. Ghislandi, E. Tkalya, C.E. Koning, G. de With, *Powder Technol.* **2012**, *221*, 351.

[37] D. Pantea, H. Darmstadt, S. Kaliaguine, C. Roy, *Appl. Surf. Sci.* **2003**, *217*, 181.

[38] X. Liu, C. Li, Y. Pan, D.W. Schubert, C. Liu, *Compos. Part B-Eng.* **2019**, *164*, 37.

[39] Z.H. Li, J. Zhang, S.J. Chen, *Express Polym. Lett.* **2008**, *2*, 695.

Graphical Abstract

M.P. Danilaev, E.A. Bogoslov, V.A. Kuklin, I.R. Vakhitov, V.G. Evtyugin, B.Z.Kamaliev, I.V. Lunev, Yu.N. Osin, A.M. Rogov, L.R. Tagirov;
Corresponding author – Maxim Danilaev* ((same order as byline))

Single-Stage Plasma-Chemical Synthesis and Characterization of Carbon Nanoparticle – Polymer Suspensions ((no stars))

ToC figure ((Please choose one size: 55 mm broad × 50 mm high **or** 110 mm broad × 20 mm high. Please do not use any other dimensions))

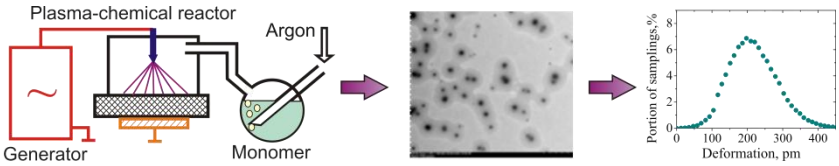

Alternating current dielectric barrier discharge (DBD) plasma allows producing of styrene polymer coatings uniformly filled with carbon nanoparticles. This single-stage synthesized armored coating demonstrates enhanced mechanical strength and resistance against conventional solvent. The transmission electron microscopy studies show carbon nanoparticles high-adhesively encapsulated by the polymer.

[399 symbols (with spaces)]